Catalysis Today 169 (2011) 217–222

Contents lists available at ScienceDirect

Catalysis Today

journal homepage: www.elsevier.com/locate/cattod

The origin of increased chemoselectivity of platinum supported on magnesium fluoride in the hydrogenation of chloronitrobenzene

Mariusz Pietrowski*, Maria Wojciechowska

Adam Mickiewicz University, Faculty of Chemistry, Grunwaldzka 6, 60-780 Poznań, Poland

ARTICLE INFO

Article history:
Available online 22 October 2010

Keywords:
Chloronitrobenzene hydrogenation
Nitrocompounds
Chloroaniline
Magnesium fluoride
Platinum catalysts

ABSTRACT

A highly active and selective catalyst for the hydrogenation of *ortho*-chloronitrobenzene (*o*-CNB) to *ortho*-chloroaniline (*o*-CAN) was obtained by supporting platinum on magnesium fluoride. In the above reaction, carried out in a liquid phase at 343 K under 3 MPa H_2, the Pt/MgF_2 catalyst was fivefold more active (apparent rate = 9.26 mol CNB/mol Pt_{surf} s) than the analogous system with Al_2O_3 as a support (apparent rate = 1.83 mol CNB/mol Pt_{surf} s). At the same time its selectivity to o-CAN (96.6%) was higher than that of Pt/Al_2O_3 (79.8%). The FTIR studies of adsorbed nitrobenzene (NB) enabled to determine the adsorption mode via oxygen atoms of nitric group. A model of o-CNB adsorption on the platinum/support interface has been proposed, according to which o-CNB adsorption proceeds on Lewis acid centres located in the vicinity of platinum crystallites which are the centres for hydrogen adsorption and dissociation. The presence of interfacial active sites was additionally proved by FTIR studies of adsorbed carbon monoxide and TPR-H_2 measurements.

1. Introduction

Substituted anilines, including halogenated anilines, are important reagents to the manufacture of a wide variety of drugs, pesticides, pigments and dyes. By way of illustration one can mention *Chlorothiazide*, which is a popular diuretic and a hypertension drug, as well as *Chlorpropham* – a herbicide belonging to the group of growth inhibitors [1].

In the past, chloroanilines were obtained by the Béchamp reduction, however, this method was abandoned for ecological reasons, because it was a source of hazardous iron oxide waste that contained toxic intermediates of the reaction. The Béchamp reduction was replaced by a catalytic method which is less environmentally burdensome, although it is not free of some drawbacks. The most important of them is the easiness at which CNB undergoes hydrodechlorination, which results in the formation of undesirable by-products, mainly aniline [2]. This fact generates serious technological problems and increases production costs associated with the separation and purification of the final product. An ideal solution of the problem would be the application of an active catalyst showing 100% selectivity to chloroaniline. Unfortunately, the catalysts used currently, such as Pt/active carbon, sulphided platinum, palladium and nickel catalysts do not reach 100% selectivity to chloroaniline, particularly at complete conversion of chloronitrobenzene [3]. Hence the interest of researchers in the search for catalysts of possibly highest selectivity. Advantageous effects were obtained by adding dehalogenation inhibitors to the reaction medium, e.g. morpholine, phosphorous acid, amines, etc. [4], as well as by using bimetallic catalysts [5–8] or colloidal nanoparticles [9–12]. Reports were also published, according to which the increase in selectivity and/or activity was achieved by applying new, untypical supports such as γ-Fe_2O_3 [13,14], SnO_2 [15], palygorskite [16], γ-ZrP [17]. The latter approach has stimulated us to investigate properties of another untypical support, namely magnesium fluoride. It is worth to add that recently a rapid increase in the number of papers on MgF_2 and its application to catalysis is observed [18–21]. Magnesium fluoride as a catalyst support was found useful in such reactions as hydrodesulphurization [22–24], hydrodechlorination [25–30], ammoxidation [31], reduction of nitrogen oxides [32,33], Knoevenagel reaction [34], oxidation of CO [35,36], photodegradation of acetone [37], and recently, hydrogenation of chloronitrobenzene to chloroaniline [38,39]. A number of MgF_2 preparation procedures were developed [18,20,40–43] and its detailed characterisation was performed [18–21]. In the present study we have used MgF_2 as a support for platinum. From among metallic, platinum shows the highest activity for the reduction of chloronitrobenzene nitric group, however its selectivity to chloroaniline is relatively low. The application of an appropriate support can result in an increase in the selectivity. The use of TiO_2 [44–46] or γ-Fe_2O_3 [13,14] leads to a considerable rise in the selectivity towards chloroaniline.

The present work was aimed at verifying the usefulness of MgF_2 as a support for platinum catalysts for chemoselective reduction of o-chloronitrobenzene to o-chloroaniline. For comparison purposes,

* Corresponding author. Fax: +48 61 8658008.
E-mail address: mariop@amu.edu.pl (M. Pietrowski).

0920-5861/$ – see front matter © 2010 Elsevier B.V. All rights reserved.
doi:10.1016/j.cattod.2010.09.021

a Pt/Al_2O_3 catalyst was employed in the study. Moreover, attempts were made at explaining the high selectivity of Pt/MgF_2 catalyst on the grounds of IR-spectroscopic investigation of adsorbed CO and nitrobenzene as well as TPR-H_2 studies.

2. Materials and methods

2.1. Preparation of supports and catalysts

Magnesium fluoride was obtained by adding small portions of $MgCO_3{\cdot}2H_2O$ to an aqueous solution of hydrofluoric acid until neutralisation followed by acidification with a few additional drops of the acid. The precipitate was then aged at room temperature for a few days under stirring, dried at 353 K and calcined at 673 K for 4 h. After the calcination, MgF_2 was ground to obtain particles of 0.2–0.5 mm in size. Platinum was deposited on MgF_2 by conventional impregnation using an aqueous solution of H_2PtCl_6. The required amount of H_2PtCl_6 was dissolved in water, then contacted with MgF_2 at room temperature for several minutes, followed by evaporation of water. The solid was dried at 353 K, then reduced at 673 K under hydrogen flow for 4 h. The Pt content was 1 wt.%. The catalysts were labelled as Pt–Mg.

Aluminium oxide was prepared by hydrolysis of aluminium isopropoxide. The obtained aluminium hydroxide was washed out of isopropyl alcohol, dried at 383 K for 24 h, then calcined at 823 K for 4 h. The Pt/Al_2O_3 (1 wt.% of Pt) catalyst was prepared in the same way as the Pt/MgF_2 catalyst and labelled as Pt–Al.

2.2. Catalyst characterisation

2.2.1. Surface area

The Brunauer–Emmet–Teller surface areas were determined by N_2 adsorption at 77 K using a Micromeritics ASAP2010 sorptometer. Total pore volume and average pore radius were determined by the Barrett–Joyner–Halenda (BJH) method using a desorption isotherm.

2.2.2. FTIR spectroscopy – CO and nitrobenzene adsorption

Fourier Transform Infrared (FTIR) studies were carried out on a Bio-Rad spectrometer, model FTS 3000MX. The samples, prepared in the form of self-supporting wafers (10 mg/cm^2), were placed in a glass cell equipped with KRS-5 windows. Before FTIR experiments, samples were evacuated *in situ* at 573 K for 1 h at 4×10^{-3} Pa to remove adsorbed water and impurities. Then the samples were cooled down for CO and benzene adsorption at room temperature.

Carbon monoxide was adsorbed at 1.3 kPa and nitrobenzene at 0.7 kPa for 10 min at 298 K. After evacuation, spectra of adsorbed species were recorded with a resolution of 4 cm^{-1}. The FTIR spectrum of a sample before adsorption was used as a subtraction background. Measurements of nitrobenzene chemisorption were carried out for platinum-free supports and for platinum catalysts at 298 K. Spectra shown in Fig. 3 were recorded after evacuation of samples at 323 K for 15 min.

2.2.3. Temperature programmed reduction – TPR-H_2

The measurements were performed on a ChemiSorb 2705 instrument made by Micromeritics. The gases used in the measurements were of high purity. The susceptibility to reduction was measured in a stream of 10 vol.% H_2 in argon. The volume rate flow of the gas mixture was 30 cm^3/min and temperature increased at the rate of 10 K/min. The calibration for the determination of hydrogen consumed was performed by introducing a specified volume of hydrogen (using a sample loop) into the stream of argon.

2.2.4. The determination of metal dispersion by hydrogen chemisorption

Prior to hydrogen chemisorption, samples were pretreated *in situ* to remove adsorbed molecules from the surface of platinum. Samples were evacuated for 15 min at room temperature and next at 673 K for 60 min, followed by reduction in hydrogen flow (40 cm^3/min) at 673 K and evacuated again for 120 min at 673 K. All chemisorption experiments were performed on an ASAP 2010C sorptometer. Chemisorption of hydrogen was carried out at 308 K and the isotherms were determined using 5 different pressures in the range of 12–40 kPa. After first set of pressures (isotherm H_t) the catalyst was evacuated at 308 K for 30 min to remove reversibly adsorbed hydrogen (H_{rev}) and the same procedure was repeated. The difference between adsorbed hydrogen extrapolated to zero pressure value for two isotherms equals to the amount of hydrogen irreversibly bound (H_{irr}).

By assuming that the stoichiometry for hydrogen adsorption on surface platinum atoms (Pt_s) is 1:1, the dispersion of platinum is given by $D = Pt_s/Pt_t = H/Pt_t$ (Pt_t – total number of platinum atoms). Platinum dispersion was calculated from irreversibly chemisorbed hydrogen.

2.3. Catalytic procedure

Hydrogenation of *ortho*-chloronitrobenzene (o-CNB) to *ortho*-chloroaniline (o-CAN) was performed in a liquid-phase at 343 K for 2 h under hydrogen pressure of 3.0 MPa in a 200 cm^3 stainless steel autoclave with a glass tube inside equipped with magnetic stirrer. The autoclave was loaded with 25 mg of catalyst and 50 cm^3 of 0.4 M methanolic solution of o-CNB. Then the autoclave was flushed several times with helium followed by flushing with hydrogen in order to remove air. In each case, the reaction time was 2 h and stirring rate was 1000 rpm. Results of the experiments show that the reaction was conducted in the absence of external mass transport limitations (the stirring rates from 800 to 1000 rpm did not affect the reaction rate). The overall molar CNB/Pt ratio was 15,600. The reaction products were analysed on a gas chromatograph equipped with a capillary column RESTEK MXT-5. Catalytic activity was expressed as a apparent rate (r) in moles of o-CNB reacted per mole of platinum (r_t) or per surface Pt atoms (r_s) (the latter value was determined by hydrogen chemisorption). Catalytic measurements carried out with platinum-free MgF_2 and Al_2O_3 supports proved the inactivity of the supports for the reduction of nitric group of o-CNB.

3. Results and discussion

3.1. Catalyst characterisation

Magnesium fluoride prepared by reacting magnesium carbonate with hydrofluoric acid is characterised by well-developed structure of mesopores as it results from type IV isotherm and H1 hysteresis loop (not shown in this paper). MgF_2 calcined for 4 h at 673 K has BET surface area of about 50 m^2/g and relatively large average pore radius (~10 nm) – Table 1. In the case of the liquid-phase reaction, where processes of mass transfer within catalyst particles play a considerable role, this fact (i.e. large pores) is an advantage. The textural characterisation of MgF_2 used in this study was presented in Table 1.

The impregnation of magnesium fluoride with aqueous solution of hexafluoroplatinic acid, followed by reduction in hydrogen flow (4 h at 673 K), results in a decrease in surface area to 35 m^2/g.

Alumina, one of the most popular supports, was chosen by us as for comparative purposes. After calcination at 823 K we have obtained γ-Al_2O_3 (proved by XRD pattern) of surface area equal to

Table 1
Textural properties of supports and catalysts.

Sample	BET surface area, m^2/g	Total pore volume, cm^3/g	Average pore radius, nm
MgF_2	50	0.33	9.8
Pt–Mg[a]	35	0.28	13.4
Al_2O_3	217	0.40	3.0
Pt–Al[b]	216	0.35	2.8

[a] 1 wt.% Pt/MgF_2.
[b] 1 wt.% Pt/Al_2O_3.

217 m^2/g. The introduction of platinum to its surface followed by 4-h reduction at 673 K practically does not affect the value of surface area.

An important parameter characterising metallic catalysts is the dispersion of metallic phase. The most frequently used techniques for the determination of metal dispersion are transmission electron microscopy, X-ray powder diffraction and chemisorption methods. In our study we have employed hydrogen chemisorption, because the amount of chemisorbed hydrogen enables to determine not only the average size of metallic particles, but also the number of platinum surface atoms required for the calculation of apparent rate (r_s) of hydrogenation reaction. We did not carried out TEM measurements because their interpretation is difficult due to relatively high electron density of MgF_2. On the other hand, XRD experiments did not show the presence of reflections originated from platinum metal, hence there was no possibility of determining platinum particle size on the ground of diffraction line broadening. However, we perfectly realise the uncertainty associated with the determination of Pt particle size only on the ground of hydrogen chemisorption (which can be retarded by strong metal–support interactions), therefore in further part of this paper we shall use the term "chemisorption capacity".

Results of hydrogen chemisorption measurements on platinum catalysts are presented in Table 2. Measurements performed on platinum-free supports (MgF_2 and Al_2O_3) have shown no capability of chemisorbing hydrogen. Volumes of hydrogen irreversibly bound on platinum supported on MgF_2 and γ-Al_2O_3 were close (0.131 and 0.115 cm^3/g, respectively). The values of metal dispersion, calculated on this ground, were 23 and 20% and metal particle sizes 5 and 6 nm, respectively. The absence of XRD reflections coming from Pt indicates that the size of platinum particles can be considerable smaller than that calculated on the grounds of hydrogen chemisorption measurements.

Studies of temperature programmed reduction were carried out on samples dried at 353 K. TPR profile of the precursor of Pt–Al catalyst (Fig. 1) is a typical profile of H_2PtCl_6 reduction with one dominant signal at about 515 K that originates from reduction of the above precursor compound. Catalysts tested in this study were reduced at 673 K. Taking this fact into consideration, the amount of hydrogen consumed in the temperature range of 298–673 K was used for calculation of the degree of platinum reduction in a catalyst. In the case of Pt–Al sample, the latter is equal to ~97%, which means that almost all platinum present in the catalyst occurs at zero oxidation state. The susceptibility of MgF_2-supported platinum precursor is considerably lower than that of Al_2O_3-supported one.

It results from TPR-H_2 experiments that almost 10% of platinum in the Pt–Mg catalyst is present in the form of unreduced species. This fact is also confirmed by the presence of strong signals of reduction observed in the range of 673–950 K. One can suppose that the above signals originate from Pt-containing species strongly interacting with MgF_2 surface and, due to this, being difficult to reduce. The shape of TPR-H_2 profile suggests the occurrence of more than one Pt–MgF_2 species of different susceptibility to reduction. It is likely that the presence of these species results from

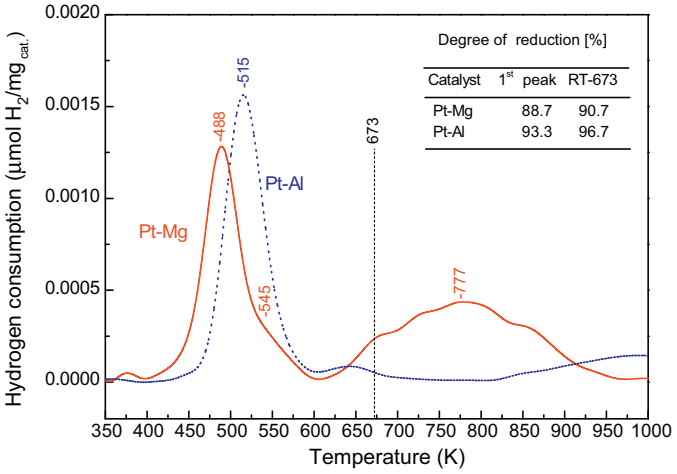

Fig. 1. TPR-H_2 profiles of Pt–Mg and Pt–Al catalysts and reduction degrees calculated on the grounds of TPR-H_2 experiments.

strong interactions between platinum and highly electronegative fluorine atoms on Pt crystallite/MgF_2 interface. The size of TPR signal at ~777 K suggests that the concentration of such species on the Pt–Mg catalyst is relatively large and this may influence its catalytic performance. The amount of these centres on the catalyst surface can be considerably greater than the mentioned 10%, which can be the reason for the observed differences in catalytic properties of Pt–Mg and Pt–Al systems.

Infrared spectra of carbon monoxide adsorbed on catalyst surfaces is often used for the characterisation of the state of metallic phase. Adsorption of CO on platinum catalysts usually results in two characteristic ν(CO) bands – one in the range 2090–2000 cm^{-1}, originated from the linear form of CO adsorbed of Pt atoms, and the other in the range 1860–1780 cm^{-1} ascribed to the adsorption of CO bridged on two Pt atoms [47]. In our study the latter band was not observed. Fig. 2A shows FTIR spectrum of carbon monoxide adsorbed at room temperature on reduced Pt–Mg catalyst and spectra recorded after CO desorption at 323, 373 and 423 K. Immediately after adsorption, two ν(CO) bands at 2116 and 2061 cm^{-1} were observed (Fig. 2A). There is agreement between researchers that vibrations of CO adsorbed on partially oxidised platinum atoms are responsible for the former band which is quite stable and resistant to evacuation at higher temperatures. The absence of the band shift during evacuation enables to conclude that the distance between the adsorption centres is large enough to prevent from dipole–dipole interactions of neighbouring CO molecules. In other words, the density of $Pt^{\delta+}$ centres is relatively low. The band at 2061 cm^{-1} behaves in a completely different way, showing on evacuation a quick shift towards lower wavenumbers, as far as 2015 cm^{-1} at 423 K. The mentioned shift is ascribed to a gradual disappearance of dipole–dipole interactions between adsorbed CO molecules. The origin of the band 2061–2015 cm^{-1} is usually sought in CO species linearly adsorbed on Pt^0 atoms [48]. A next band appears at 2035 cm^{-1} only after evacuation at 323 K and undergoes a gradual shift to lower wavenumbers with the decrease of CO coverage of platinum atoms (to 1983 cm^{-1} at 423 K) as a result of vanishing of dipole–dipole interactions between CO molecules.

After evacuation at 423 K, the band discussed above becomes a dominant one. The interpretation of this band is not as unambiguous as that of the two bands mentioned previously. It can originate from CO linearly adsorbed on Pt sites of low or extremely low coordination or even from CO adsorbed on Pt sites perturbed by direct interaction with the support [49,50]. We are inclined to the latter of the interpretations although, in our opinion, further detailed studies of CO adsorption on Pt/MgF_2 catalysts are necessary to find

Table 2
Hydrogen chemisorption on platinum catalysts.

Sample	Volume adsorbed, cm^3/g			Dispersion, %	
	Total (H_t)	Irreversible (H_{irr})	Reversible (H_r)	Total (D_t)	Irreversible (D_{irr})
Pt–Mg	0.193	0.131	0.062	33.6	22.8
Pt–Al	0.177	0.115	0.062	30.8	20.0

a final solution of the problem. We can assume with a high probability that platinum occurs on the surface of Pt–Mg catalysts at zero oxidation state (Pt^0) and as partially oxidized species $Pt^{\delta+}$. One can put forward a working hypothesis that $Pt^{\delta+}$ centres are generated as a result of interactions between platinum and highly electronegative fluoride ions of the support, which at the same time explains strong metal–support interactions and the presence of hard-to-reduce platinum species observed in TPR studies.

In the spectrum of CO adsorbed on Pt–Al catalyst (Fig. 2B), only a broad band at 2048–1995 cm^{-1} was observed, which points to the presence of Pt^0 atoms. On evacuation, contrary to Pt–Mg catalyst, no band at a lower frequency appears, which should be interpreted as the absence of strong interactions between Pt and Al_2O_3 surface.

3.2. Catalytic activity

Activity and selectivity of Pt–Mg and Pt–Al catalysts were listed in Table 3.

In spite of applying the same method of platinum mounting on both supports and almost identical hydrogen chemisorption capacity, Pt–Mg and Pt–Al catalysts differ considerably in their activity and selectivity. The platinum catalyst supported on MgF_2 is almost six times more active for the reduction of nitric group of o-CNB and its selectivity to o-CAN is close to 97%. This fact is worth of paying particular attention since usually high selectivity does not accompany high activity. The selectivity of 97% observed in the case of Pt–Mg catalyst should be also emphasised because it was obtained for a typical metallic catalyst prepared by a simple impregnation method. The catalysts did not contain any modifiers and consisted of active phase and support only. Of course, catalysts of a higher selectivity were reported in the literature, however they are usually modified by the introduction of a number of additives which considerably complicates catalyst preparation and makes it more expensive. This is why our Pt–Mg catalyst is a perfect material for further studies orientated towards obtaining 100% selectivity to o-CAN.

The presented results show that catalytic properties of platinum are substantially modified by metal–support interactions in the Pt/MgF_2 system. The number of metallic centres on surfaces of Pt–Mg and Pt–Al catalysts is almost identical. Therefore one can assume that the accessibility of the centres to hydrogen is comparable as well, which was confirmed by results of chemisorption measurements. Why in such a case such great differences are observed in activity and selectivity of both catalysts? In our opinion, the reason for the differences should be sought in the presence of specific adsorption centres on the surface of Pt–Mg catalyst.

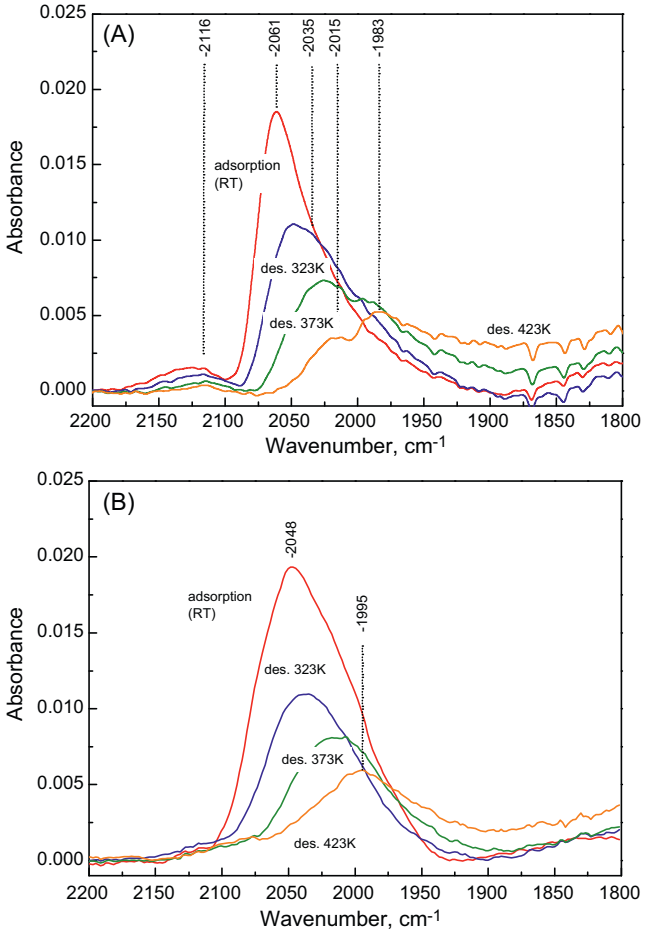

Fig. 2. FTIR spectra of adsorbed carbon monoxide on Pt–Mg catalyst (A), and Pt–Al catalyst (B).

3.3. FTIR study of chemisorbed nitrobenzene

Measurements of *ortho*-chloronitrobenzene chemisorption are very difficult to perform because this compound is a solid at room temperature. This is why we have used in this study a simpler molecule – nitrobenzene (NB), assuming that chloronitrobenzene can adsorb in the way similar to that of nitrobenzene.

After NB adsorption on the samples examined, characteristic bands originated from stretching vibrations of nitric group, asymmetric $\nu_{as}(NO)$ and symmetric $\nu_s(NO)$ vibrations as well as C–C vibrations of aromatic ring were observed (Fig. 3).

Spectra of NB adsorbed on Al_2O_3 and on Pt–Al catalyst are very similar to the spectrum of liquid phase nitrobenzene and are in agreement with literature data for NB adsorption on the surface of Al_2O_3 [51,52]. Wavenumbers of bands originated from C–C stretching vibrations in aromatic ring are exactly the same as those reported in the literature [53] for liquid NB, which points to the absence of interactions between the ring and sample surface [54]. Moreover, it is confirmed by the lack of shifts of bands coming

Table 3
Activity and selectivity of platinum catalysts in the reaction of selective reduction of o-CNB to o-CAN.

Sample	Apparent rate, r_t[a] (mol_{CNB}/mol_{Pt} s)	Apparent rate, r_s[b] (mol_{CNB}/mol_{Pt} s)	Selectivity, %
Pt–Mg	2.14	9.26	96.6
Pt–Al	0.36	1.83	79.8

[a] r_t – apparent rate values calculated for the total Pt content in a catalyst (1 wt.%).
[b] r_s – apparent rate values calculated for surface platinum atoms (determined by hydrogen chemisorption).

Table 4
Positions of bands ascribed to stretching vibrations ν(NO) of liquid phase nitrobenzene NO_2 group and after nitrobenzene adsorption on surfaces of supports and catalysts.

Sample	1 ν_{as}(NO)	2 $\Delta\nu_{as}$(NO)	3 ν_s(NO)	4 $\Delta\nu_s$(NO)	5 $I\nu_{as}/I\nu_s$
NB-lq [53]	1523	–	1347	–	0.95
Al_2O_3	1525	+2	1350	+3	0.86
Pt–Al	1525	+2	1350	+3	0.83
MgF_2	1529	+6	1369	+22	1.54
Pt–Mg	1528	+5	1366	+19	1.22

Columns 2 and 4 – band shift in relation to liquid phase NB. Column 5 – intensity ratios of ν_{as}(NO)/ν_s(NO) bands.

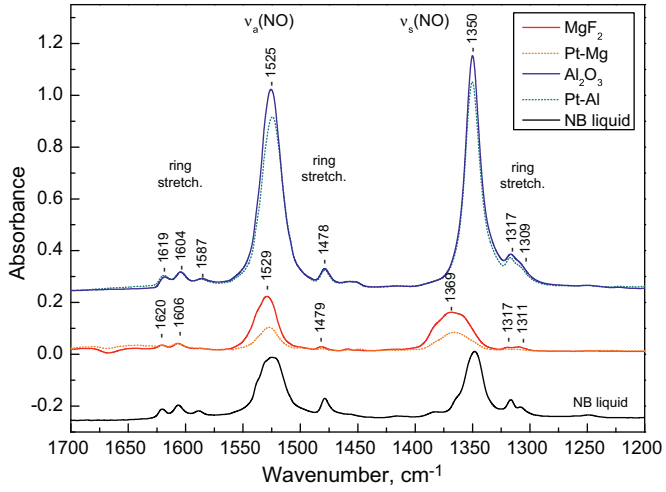

Fig. 3. FTIR spectra in the fingerprint region of nitrobenzene adsorbed on MgF_2 and Al_2O_3 supports as well as on Pt–Mg and Pt–Al catalysts.

from C–H stretching vibrations in the region of 3000–3200 cm^{-1} (not shown). Small shifts towards higher wavenumbers were, however, observed in the case of bands originated from N–O stretching vibrations of nitric group, which proves the participation of this group in NB adsorption. Wavenumbers of bands, their shifts and intensity ratios were listed in Table 4. The change in intensities of ν_{as}(NO)/ν_s(NO) bands (column 5 in Table 4) also testifies for the occurrence of NB adsorption via nitric group. For liquid nitrobenzene the ratio is 0.95, whereas for NB adsorbed on Al_2O_3 and Pt–Al catalyst it decreases to 0.86 and 0.83, respectively. It should be interpreted as a result of a reduction in O–N–O bond angle in nitric group [55].

Spectra of NB adsorbed on MgF_2 and Pt–Mg differ quite clearly from those taken after NB adsorption on Al_2O_3 and Pt–Al. In the former case, band intensities are considerably lower which points to a smaller concentration of NB surface species. Also the difference between band intensities recorded for the support alone and Pt–Mg catalyst is considerably greater. One can suppose that a part of NB adsorption centres was blocked after the introduction of the active phase. While comparing with liquid phase NB, no significant differences were found in positions of bands originated from aromatic ring C–C vibrations and C–H stretching vibrations, which rules out planar adsorption of nitrobenzene via aromatic ring. On the other hand, shifts in N–O stretching vibrations of nitric group are in the case of MgF_2 support and Pt–Mg catalyst considerably greater than in the case of Al_2O_3 and Pt–Al catalyst (Table 4). The shifts reach a few cm^{-1} for ν_{as}(NO) vibrations and about +20 for ν_s(NO) vibrations. With a high certainty, these differences can be ascribed to a strong perpendicular NB adsorption via oxygen atoms of nitric group.

Considerable damping of symmetric vibrations ν_s(NO) indicates a stronger adsorption via one of oxygen atoms belonging to nitric group. Additional information on NB adsorption is provided by analysis of the shape of ν(NO) bands. Complex structure of the bands is clearly seen, particularly in the case of ν_s(NO) band which consists of as much as three components. It proves a considerable heterogeneity of adsorption centres on surfaces of MgF_2 support and Pt–Mg catalyst. In the case of Al_2O_3 and Pt–Al catalyst, analogous bands were single and symmetrical ones which indicates the presence of only one type of nitrobenzene adsorption centres. Of particular interest are band intensity ratios ν_{as}/ν_s of nitric group, which are equal to 1.54 and 1.22 for MgF_2 and Pt–Mg catalyst. Such high values reflect an increase in O–N–O bond angle in the nitric group of nitrobenzene [55].

4. Conclusions

We have found that platinum supported on MgF_2 is more active and more selective catalyst for hydrogenation of o-chloronitrobenzene to o-chloroaniline than platinum supported on Al_2O_3. In our opinion, adsorption centres for NB are Lewis acid sites of the support (coordinatively unsaturated magnesium ions), located in close neighbourhood of platinum particles. The participation of active centres present on support surface was postulated by Corma et al., who studied hydrogenation of nitrostyrene nitric group on titania-supported gold catalyst [54] and recently also by Shimizu et al. [51]. Nitrobenzene adsorption centres on MgF_2 surface are characterised by a considerable heterogeneity and among them active sites of optimal acid strength and geometry which create favourable conditions for hydrogenation of nitric group. Some role in the formation of catalytic properties can be played by the centres on the MgF_2/Pt interface, which seem to be partially oxidised platinum atoms $Pt^{\delta+}$, generated as a result of the interaction with strongly electronegative fluoride ions.

Results presented in this study cast some light on the source of activity and selectivity of Pt/MgF_2 catalyst for hydrogenation of nitric group of chloronitrobenzene. However, the subject is far from being exhausted and further studies are continued.

References

[1] M. Bohnet, Ullmann's Encyclopedia of Industrial Chemistry, Wiley–VCH, 2003.
[2] R.L. Augustine, Heterogeneous Catalysis for the Synthetic Chemist, CRC Press, 1996.
[3] S. Nishimura, Handbook of Heterogeneous Catalytic Hydrogenation for Organic Synthesis, Wiley–Interscience, 2001.
[4] X. Wang, M. Liang, J. Zhang, Y. Wang, Curr. Org. Chem. 11 (2007) 299.
[5] B. Coq, F. Figueras, Coord. Chem. Rev. 180 (1998) 1753.
[6] Z. Yu, S. Liao, Y. Xu, B. Yang, D. Yu, J.A.C.S., Chem. Commun. (1995) 1155.
[7] K.N. Rao, B.M. Reddy, S.E. Park, Catal. Commun. 11 (2009) 142.
[8] X.X. Han, R.X. Zhou, G.H. Lai, X.M. Zheng, Catal. Today 93–95 (2004) 433.
[9] W.W. Yu, H.F. Liu, J. Mol. Catal. A: Chem. 243 (2006) 120.
[10] W.X. Tu, B.L. He, H.F. Liu, X.L. Luo, X. Liang, Chin. J. Polym. Sci. 23 (2005) 211.
[11] W.X. Tu, H.F. Liu, Y. Tang, J. Mol. Catal. A: Chem. 159 (2000) 115.
[12] M.H. Liu, W.Y. Yu, H.F. Liu, J. Mol. Catal. A: Chem. 138 (1999) 295.
[13] J.L. Zhang, Y. Wang, H. Ji, Y.G. Wei, N.Z. Wu, B.J. Zuo, Q.L. Wang, J. Catal. 229 (2005) 114.
[14] M.H. Liang, X.D. Wang, H.Q. Liu, H.C. Liu, Y. Wang, J. Catal. 255 (2008) 335.
[15] B.J. Zuo, Y. Wang, Q.L. Wang, J.L. Zhang, N.Z. Wu, L.D. Peng, L.L. Gui, X.D. Wang, R.M. Wang, D.P. Yu, J. Catal. 222 (2004) 493.
[16] F. Wang, J.H. Liu, Y.Q. Yin, X.L. Xu, Wuli Huaxue Xuebao 25 (2009) 1678.
[17] F. Wang, J. Liu, X. Xu, Chem. Commun. (2008) 2040.

[18] S. Wuttke, S.M. Coman, G. Scholz, H. Kirmse, A. Vimont, M. Daturi, S.L.M. Schroeder, E. Kemnitz, Chem. Eur. J. 14 (2008) 11488.
[19] M. Nickkho-Amiry, G. Eltanany, S. Wuttke, S. Rüdiger, E. Kemnitz, J.M. Winfield, J. Fluor. Chem. 129 (2008) 366.
[20] M. Wojciechowska, M. Zieliński, M. Pietrowski, J. Fluor. Chem. 120 (2003) 1.
[21] J. Krishna Murthy, U. Groß, S. Rüdiger, E. Kemnitz, J.M. Winfield, J. Solid State Chem. 179 (2006) 739.
[22] M. Wojciechowska, M. Pietrowski, B. Czajka, S. Lomnicki, Catal. Lett. 87 (2003) 153.
[23] M. Wojciechowska, M. Pietrowski, B. Czajka, Catal. Today 65 (2001) 349.
[24] M. Wojciechowska, M. Pietrowski, S. Lomnicki, Chem. Commun. (1999) 463.
[25] A. Malinowski, W. Juszczyk, J. Pielaszek, M. Bonarowska, M. Wojciechowska, Z. Karpiński, Stud. Surf. Sci. Catal. 130C (2000) 1991.
[26] A. Malinowski, W. Juszczyk, J. Pielaszek, M. Bonarowska, M. Wojciechowska, Z. Karpiński, Chem. Commun. (1999) 685.
[27] A. Malinowski, W. Juszczyk, M. Bonarowska, M. Wojciechowska, Z. Kowalczyk, Z. Karpiński, React. Kinet. Catal. Lett. 68 (1999) 53.
[28] H. Berndt, H. Bozorg Zadeh, E. Kemnitz, M. Nickkho-Amiry, M. Pohl, T. Skapin, J.M. Winfield, J. Mater. Chem. 12 (2002) 3499.
[29] I.K. Murwani, E. Kemnitz, T. Skapin, M. Nickkho-Amiry, J.M. Winfield, Catal. Today 88 (2004) 153.
[30] Y.C. Cao, X.Z. Jiang, J. Mol. Catal. A: Chem. 242 (2005) 119.
[31] V.N. Kalevaru, B. David Raju, V. Venkat Rao, A. Martin, Appl. Catal. A: Gen. 352 (2009) 223.
[32] J. Haber, M. Wojciechowska, M. Zieliński, W. Przystajko, Catal. Lett. 113 (2007) 46.
[33] M. Wojciechowska, M. Zieliński, J. Goslar, A. Malczewska, W. Przystajko, Pol. J. Chem. 74 (2000) 1321.
[34] R.M. Kumbhare, M. Sridhar, Catal. Commun. 9 (2008) 403.
[35] M. Ruszel, B. Grzybowska, M.A. Małecka, L. Kępiński, J. Sobczak, M. Wojciechowska, Pol. J. Chem. 83 (2009) 1185.
[36] M. Wojciechowska, I. Tomska-Foralewska, W. Przystajko, M. Zieliński, Catal. Lett. 104 (2005) 121.
[37] F. Chen, T.H. Wu, X.P. Zhou, Catal. Commun. 9 (2008) 1698.
[38] M. Pietrowski, M. Zieliński, M. Wojciechowska, Catal. Lett. 128 (2009) 31.
[39] M. Pietrowski, M. Wojciechowska, Catal. Today 142 (2009) 211.
[40] M. Pietrowski, M. Wojciechowska, J. Fluor. Chem. 128 (2007) 219.
[41] M. Wojciechowska, A. Wajnert, I. Tomska-Foralewska, M. Zieliński, B. Czajka, Catal. Lett. 128 (2009) 77.
[42] S. Wuttke, G. Scholz, S. Rüdiger, E. Kemnitz, J. Mater. Chem. 17 (2007) 4980.
[43] U. Groß, S. Rüdiger, E. Kemnitz, Solid State Sci. 9 (2007) 838.
[44] B. Coq, A. Tijani, R. Dutartre, F. Figueras, J. Mol. Catal. 79 (1993) 253.
[45] F. Cárdenas-Lizana, S. Gómez-Quero, M.A. Keane, ChemSusChem 1 (2008) 215.
[46] F. Cárdenas-Lizana, S. Gómez-Quero, N. Perret, M.A. Keane, Gold Bull. 42 (2009) 124.
[47] P. Bazin, O. Saur, J.C. Lavalley, M. Daturi, G. Blanchard, PCCP 7 (2005) 187.
[48] V. Perrichon, L. Retailleau, P. Bazin, M. Daturi, J.C. Lavalley, Appl. Catal. A: Gen. 260 (2004) 1.
[49] M.J. Kappers, J.H. Vandermaas, Catal. Lett. 10 (1991) 365.
[50] G.D. Zhang, B. Coq, L.C. deMenorval, D. Tichit, Appl. Catal. A: Gen. 147 (1996) 395.
[51] K. Shimizu, Y. Miyamoto, T. Kawasaki, T. Tanji, Y. Tai, A. Satsuma, J. Phys. Chem. C 113 (2009) 17803.
[52] C.A. Koutstaal, P. Angevaare, E.J. Grootendorst, V. Ponec, J. Catal. 141 (1993) 82.
[53] J. Clarkson, W.E. Smith, J. Mol. Struct. 655 (2003) 413.
[54] M. Boronat, P. Concepción, A. Corma, S. González, F. Illas, P. Serna, J. Am. Chem. Soc. 129 (2007) 16230.
[55] I. Ahmad, T.J. Dines, C.H. Rochester, J.A. Anderson, J. Chem. Soc., Faraday Trans. 92 (1996) 3225.